Neurotherapeutics (2021) 18:1748–1767
https://doi.org/10.1007/s13311-021-01044-3

ORIGINAL ARTICLE

Oleoylethanolamide Delays the Dysfunction and Death of Purkinje Cells and Ameliorates Behavioral Defects in a Mouse Model of Cerebellar Neurodegeneration

Ester Pérez-Martín[1,2] · Rodrigo Muñoz-Castañeda[1,2] · Marie-Jo Moutin[3] · Carmelo A. Ávila-Zarza[2,4] · José M. Muñoz-Castañeda[5] · Carlos Del Pilar[1,2] · José R. Alonso[1,2,6] · Annie Andrieux[3] · David Díaz[1,2] · Eduardo Weruaga[1,2]

Accepted: 16 March 2021 / Published online: 7 April 2021

Abstract

Oleoylethanolamide (OEA) is an endocannabinoid that has been proposed to prevent neuronal damage and neuroinflammation. In this study, we evaluated the effects of OEA on the disruption of both cerebellar structure and physiology and on the behavior of Purkinje cell degeneration (PCD) mutant mice. These mice exhibit cerebellar degeneration, displaying microtubule alterations that trigger the selective loss of Purkinje cells and consequent behavioral impairments. The effects of different doses (1, 5, and 10 mg/kg, i.p.) and administration schedules (chronic and acute) of OEA were assessed at the behavioral, histological, cellular, and molecular levels to determine the most effective OEA treatment regimen. Our *in vivo* results demonstrated that OEA treatment prior to the onset of the preneurodegenerative phase prevented morphological alterations in Purkinje neurons (the somata and dendritic arbors) and decreased Purkinje cell death. This effect followed an inverted U-shaped time-response curve, with acute administration on postnatal day 12 (10 mg/kg, i.p.) being the most effective treatment regimen tested. Indeed, PCD mice that received this specific OEA treatment regimen showed improvements in motor, cognitive and social functions, which were impaired in these mice. Moreover, these *in vivo* neuroprotective effects of OEA were mediated by the PPARα receptor, as pretreatment with the PPARα antagonist GW6471 (2.5 mg/kg, i.p.) abolished them. Finally, our *in vitro* results suggested that the molecular effect of OEA was related to microtubule stability and structure since OEA administration normalized some alterations in microtubule features in PCD-like cells. These findings provide strong evidence supporting the use of OEA as a pharmacological agent to limit severe cerebellar neurodegenerative processes.

Keywords Cerebellum · Endocannabinoid · Neurodegeneration · Neuroprotection · OEA · Purkinje cell

Introduction

Microtubule defects are known to be the basis of several brain diseases [1–9], even causing the death of neural populations [10–13]. Recently, we showed that excess polyglutamylation induces alterations in both the dynamics and structure of microtubules in Purkinje cell degeneration (PCD) mice [9, 10, 13, 14]. These animals harbor a mutation in the *Nna1/Ccp1* gene, which encodes carboxypeptidase 1 (CCP1), an enzyme responsible for the deglutamylation of microtubules. A lack of activity of this enzyme triggers

These authors Ester Pérez-Martín and Rodrigo Muñoz-Castañeda contributed equally to this work.

✉ David Díaz
ddiaz@usal.es

✉ Eduardo Weruaga
ewp@usal.es

1 Laboratory of Neuronal Plasticity and Neurorepair, Institute for Neurosciences of Castile and Leon (INCyL), University of Salamanca, 37007 Salamanca, Spain

2 Institute of Biomedical Research of Salamanca (IBSAL), 37007 Salamanca, Spain

3 GIN, Univ. Grenoble Alpes, CNRS, CEA, Grenoble Institute Neurosciences, Inserm, U121638000 Grenoble, France

4 Department of Statistics, University of Salamanca, 37007 Salamanca, Spain

5 Department of Theoretical, Atomic and Optical Physics, University of Valladolid, 47071 Valladolid, Spain

6 Universidad de Tarapacá, Arica, Chile

excessive microtubule polyglutamylation and subsequent postnatal Purkinje cell death [10, 13]. The neuronal degeneration caused by the loss of CCP1 activity is a complex process involving two clearly distinct phases: a preneurodegenerative stage from postnatal day (P) 15 to P18, which is characterized by nuclear, cytological, and morphological alterations in Purkinje cells, and a neurodegenerative stage from P18 onwards, in which Purkinje cells die [14–16]. Purkinje cell degeneration at these ages contributes not only to motor dysfunction but also to gradual cognitive and social impairments in PCD mice throughout the cerebellar degeneration process, as has been reported in other models in which the cerebellum is affected [14, 17–19]. During preneurodegeneration, the exploratory and social behaviors of PCD mutants on C57BL/DBA background are affected, showing less rearing time and a lack of social preference compared to wild-type (WT) animals [14, 20]. From the beginning of the neurodegeneration stage, PCD mutants were impaired in motor tasks, grooming behavior and memory recognition, showing lower fall latency in the *rotarod* test, differences in the time spent in grooming and a lack of novelty discrimination compared to the behavior of WT mice [14, 19]. This animal model recapitulates key features of the infantile-onset neurodegeneration and cerebellar atrophy observed in humans with a monogenic biallelic mutation in *CCP1* [7, 21]. Thus, the PCD mutant mouse is a very suitable model for exploring and assessing different therapeutic approaches for treating severe human degenerative disorders.

The endocannabinoid system plays an essential role in microtubule-related brain diseases, and some of its components have been reported to exert neuroprotective effects [22–25]. However, to our knowledge, there have been no studies addressing the use of noncanonical endocannabinoids as therapeutic agents for the treatment of these neurodegenerative diseases. In this sense, the endocannabinoid oleoylethanolamide (OEA) has been shown to prevent neuronal damage and neuroinflammation in different animal models of brain disease and mental disorders [26–34]. Moreover, the binding of OEA to peroxisome proliferator-activated receptor-alpha (PPARα) [35–38] triggers the expression of different microtubule-associated proteins that may influence the stability of microtubules, preventing neurons from degenerating [39]. Thus, OEA has emerged as a promising therapeutic agent for preventing microtubule-related neurodegeneration and reversing subsequent neurobehavioral impairments.

Therefore, the objective of this work was to examine the effect of OEA on cerebellar degeneration and neurobehavioral defects in PCD mice. To this end, we analyzed the general cerebellar structure and the morphology and survival of Purkinje cells after administering OEA at different dosages to PCD mice *in vivo*. Then, we explored the effect of OEA on motor, cognitive and social functions, which are impaired in this animal model. Additionally, we assessed the involvement of PPARα receptors in the effects of OEA observed *in vivo*. Finally, we employed an additional *in vitro* model to identify the cellular mechanisms triggered by OEA, which could not be properly analyzed *in vivo*. To this end, we examined microtubule dynamics and structure in *Ccp1*-KO cells by exposing them to different doses of OEA.

Materials and Methods

Animals

Mice were housed under a 12-h/12-h light/dark cycle at a constant room temperature and humidity and provided *ad libitum* access to water and special rodent chow at the Animal Facilities of the University of Salamanca (Salamanca, Spain) or Joseph Fourier University (Grenoble, France). All animal procedures were approved by Bioethics Committees of both the University of Salamanca and Joseph Fourier University and were performed in accordance with the guidelines established by European (2010/63/UE) and national legislations (Spanish RD53/2013 and Law 32/2007; French permit no. 38 07 11). All efforts were made to minimize animal suffering and to use the fewest animals required to produce statistically relevant results.

WT and mutant *pcd*^{1J} (PCD) mice on a C57BL/DBA background were obtained from Jackson Labs and employed for all the *in vivo* procedures, and WT and *Ccp1*-KO mouse embryos were used to isolate cells for the *in vitro* experiments. *Ccp1*-KO mice are considered equivalent to the standard PCD mouse model since like PCD mice, they lack the expression of *Ccp1* mRNA [10, 14]. The procedures for *Ccp1*-KO-derived cell culture and subsequent *in vitro* analyses (see below) were standardized at Joseph Fourier University to ensure the feasibility of these experiments.

The *in vivo* or *in vitro* studies are described separately below.

In vivo Studies

In vivo Experimental Design

To facilitate the presentation of the *in vivo* procedures performed in this study, we provide a summary of the workflow, experimental groups and sample size for each set of experiments below.

1. Before the start of the *in vivo* OEA experiments, the expression of the endocannabinoid PPARα receptor in WT and PCD mice during postnatal development period was measured since PPARα is considered the main receptor through which OEA exerts its action [33].

Animals were sorted on the basis of genotype (WT or PCD) and age at analysis (P7, P15, P17, P22, or P30; $n=4$ animals per group).

2. To assess the effect of OEA treatment at the histological level, a different set of animals was employed and analyzed at P30. The experiments were divided into two phases, as depicted in Fig. 1. In the first set of experiments (Fig. 1, *Phase I*) we aimed to determine the best drug dose (0, 1, 5, or 10 mg/kg) and schedule of administration (chronically from P7 to P21 or acutely at P14 or P16, which is one day before or one day after the preneurodegenerative process begins, respectively; $n=4$ animals per group) to identify the optimal therapeutic dosage of OEA. Based on the results obtained, we performed a second experiment (Fig. 1, *Phase II*) in which we refined the critical therapeutic window of OEA by acutely administering the most effective dose (10 mg/kg, see results) of OEA at three different ages: P14, P12 and P10 (i.e., one, three and five days before the onset of preneurodegeneration in PCD mice, respectively; $n=7$ animals per group). We employed untreated PCD mice as controls in both experiments ($n=4$–7 animals).
3. To verify whether the neuroprotective effect of OEA in PCD mice also translates to an improvement in behavior, WT and untreated and treated PCD mice ($n=8$–9 animals per group) were subjected a wide set of behavioral tasks (described in detail later). To reduce the number of animals, only the most effective OEA treatment regimen was used based on the histological analyses described above. Moreover, the groups of animals subjected to behavioral tests were also employed for histological evaluation of the long-term effect of OEA treatment at P40.
4. Finally, to confirm the direct involvement of PPARα receptors in the observed *in vivo* OEA effects at both the histological and behavioral levels, an additional group of PCD mice was pretreated with the PPARα antagonist GW6471 and analyzed at P30 ($n=7$ animals).

The detailed *in vivo* experimental methodology is described below.

Drug Administration

Both OEA (Calbiochem, San Diego, USA) and the PPARα antagonist GW6471 (Tocris Bioscience, Bristol, UK) were freshly prepared on the day of administration to avoid drug degradation. Both compounds were dissolved separately in 100% ethanol v/v and diluted in H_2O Elix. OEA was administered by intraperitoneal injection (i.p.) at a dose of 1, 5 or 10 mg/kg b.w. according to previous studies [26, 28, 29]. When GW6471 was required, it was administered i.p. at a dose of 2.5 mg/kg b.w. 15 min before OEA treatment. PCD control animals were injected i.p. with 0.9% NaCl w/v. All animals were treated in the morning. The body weight of each animal was monitored throughout the entire experiment because OEA has anorexigenic side effects [35, 38, 40].

Tissue Extraction and Preparation

Animals were deeply anesthetized at P7, P15, P17, P22, P30, or P40 (depending on the experiment) with 10 µl/g b.w. chloral hydrate (Prolabo, Fontenay-sous-Bois, France) and intracardially perfused with 0.9% NaCl w/v followed by 5 ml/g b.w. modified Somogyi's fixative consisting of 4%

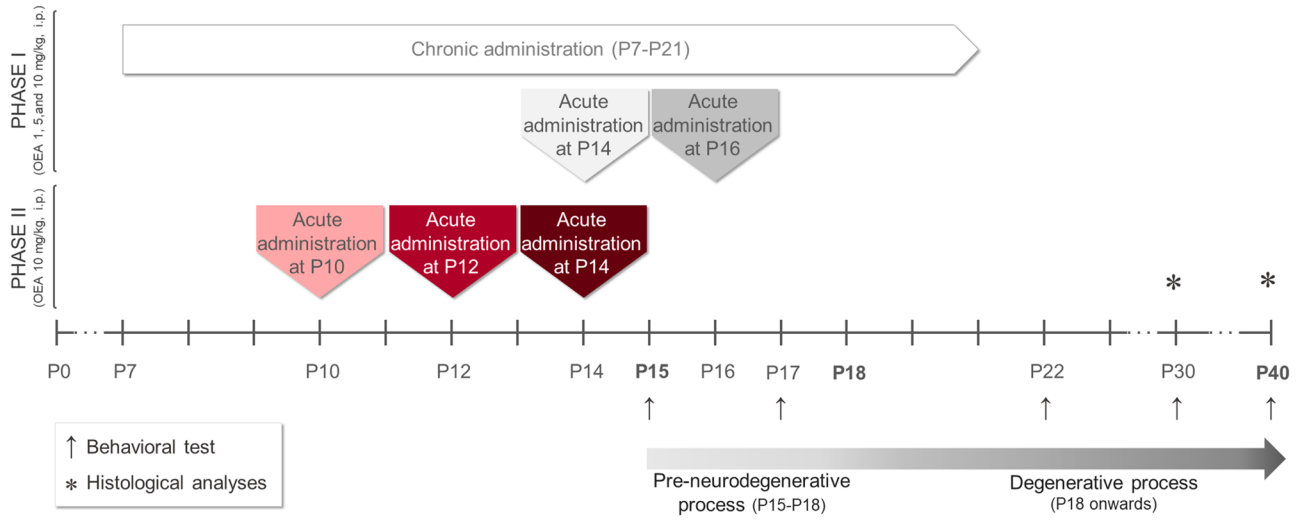

Fig. 1 The experimental *in vivo* paradigm. The timeline details the two sets of experiments of the OEA treatment, the time points for behavioral testing and tissue collection, and their relationship with the neurodegenerative process of the PCD mouse

paraformaldehyde w/v. Cerebella were sectioned sagittally using a freezing-sliding microtome (Leica Jung SM 2000, Nussloch, Germany; 30 µm thick) and washed in phosphate-buffered saline (PBS), pH 7.4.

Immunofluorescence

Free-floating sections were incubated at 4°C for 72 h under continuous rotation in 0.2% Triton X-100 v/v, 5% normal serum v/v and the following primary antibodies diluted in PBS: guinea pig anti-CB1 (1:1,000; Frontier Institute, Hokkaido, Japan), rabbit anti-PPARα (1:100; Pierce Antibodies, Rockford, IL, USA), and mouse anti-calbindin D-28k (Cb28k; 1:1000; Swant, Bellinzona, Switzerland). The following primary antibodies were employed for complementary analyses: goat anti-CB2 (1:500, Santa Cruz Biotechnology, Dallas, TX, USA) and mouse anti-S100 (1:500; Sigma-Aldrich, St. Louis, MO, USA). Different combinations of these antibodies were used for each experiment. Then, the sections were incubated with appropriate secondary antibodies conjugated to Cy2, Cy3, or Cy5 (1:500; Jackson Laboratories, West Grove, PA, USA) for 2 h at room temperature and counterstained with DAPI (1:10,000; Sigma-Aldrich) to identify the cell nuclei. For all histological analyses, four equidistant vermis parasagittal sections were assessed for each mouse.

Quantification of the Endocannabinoid PPARα

The percentage of Purkinje cells expressing PPARα in parasagittal sections of the vermis during postnatal cerebellar development (P7, P15, P17, P22, and P30) was analyzed by immunostaining for both PPARα and Cb28k. Only Purkinje cells with clear Cb28k+ somata and complete nuclei stained with DAPI were counted to avoid biases. Additionally, changes in the percentage of these cells expressing PPARα in PCD mice were evaluated after OEA treatment at P30.

Density and Morphological Analyses of Purkinje Cells

Both analyses were performed on parasagittal sections of the vermis immunostained for Cb28k. Only Purkinje cells with clear Cb28k+ somata and dendritic arbors and complete nuclei stained with DAPI were analyzed to avoid planimetric biases. Purkinje cell survival was expressed as the Purkinje cell linear density, which was calculated as the number of Purkinje cell somata per mm of the Purkinje cell layer (from lobule I to lobule X of the vermis) in each section. Then, the following morphological parameters were analyzed: (1) soma area, (2) length of Purkinje cell dendritic arbors (i.e., molecular layer thickness), and (3) length and (4) width of the primary dendrite. These analyses were performed at both P30 and P40 and carried out using Neurolucida (MBF Bioscience, Williston, Vermont, USA) and ImageJ (NIH, USA) software, as previously described [14].

Behavioral Analyses

A battery of tests of behaviors associated with cerebellar function was performed at P15, P17, P22, P30, and P40 between 9:00 am and 1:00 pm. Video recordings were obtained and meticulously analyzed by a researcher blinded to the experimental conditions (E P-M). After each trial, the various apparatuses and objects were cleaned with 70% ethanol v/v.

The *rotarod test* (Panlab, Barcelona, Spain) was used to assess motor coordination as previously described [14]. The rod accelerated at a rate of 0.06 rpm/s from 4 to 40 rpm for 10 min (rod diameter = 30 mm). The latency to fall off was measured in seven trials per day with 20-min intervals between trials. The mean latency was calculated for each mouse on each day of the task.

Home-cage behavior analysis was used to characterize general behavior [14]. After 10 min of habituation, grooming time (innate stereotyped behavior), rearing time (environmental exploratory behavior), time spent moving (general movement), time in activity and resting time were analyzed. Each animal was assigned to an individual home cage to avoid the influence of odor emitted from the other animals.

The *novel object recognition (NOR) test* was performed to evaluate long-term object recognition memory in rodents [41, 42]. On the first day (P15), two identical objects placed in opposite corners of a cage were presented to a single animal for 10 min. Then, in each of the following sessions (at P17, P22, P30, and P40), the animals were returned to the cage, which contained the familiar object and a novel one. All objects were made of plastic and were of different colors and shapes but of similar size. Two different measures of discriminatory behavior were analyzed. The first measure was the percentage of time exploring the novel (T_N) and familiar (T_F) objects, which was calculated as follows:

$$\%T_N = \frac{T_N}{T_N+T_F}, \%T_F = \frac{T_F}{T_N+T_F}.$$

The second measure was the discriminatory index (DI), which was calculated as follows:

$$DI = \frac{T_N - T_F}{T_N+T_F}.$$

The DI can vary between +1 and −1, with a positive score indicating more time spent exploring the novel object, a negative score indicating more time spent exploring the familiar object, and zero indicating a lack of preference [43].

The *three-chambered social preference test* was performed to assess sociability in a white Plexiglas box (50 × 29 cm) divided into three connected chambers [14, 44]. After 10 min of habituation, each mouse was placed in the three-chambered box containing either a mouse of the same age and sex or an object, both of which covered by a similar drilled pencil cup and placed in each of the lateral rooms of the box. The results were expressed as two different measures of sociability and preference. The first was the percentage of time spent interacting with the animal (T_A) and the object (T_O), which was calculated as follows:

$$\%T_A = \frac{T_A}{T_A+T_O}, \%T_O = \frac{T_O}{T_A+T_O}.$$

Analogous to the DI, the sociability index (SI) was calculated as follows:

$$SI = \frac{T_A - T_O}{T_A+T_O}.$$

In this case, the SI can also vary between +1 and −1, with a positive score indicating a preference for social interaction, a negative score indicating an avoidance of social interaction and zero indicating the lack of any preference concerning socialization.

In vitro Study

Cell Culture and Transfection

To study whether the effect of OEA is related to changes in microtubule stability, which is affected in PCD cells, we employed a standardized *in vitro* system based on mouse embryonic fibroblasts (MEFs) since this approach allows visualization of individual microtubules and measurement of parameters related to their morphology and dynamics [14]. The cell culture and transfection techniques required for these analyses compromise the viability of PCD-derived neurons and thus the ability to obtain reliable data [14]. For this reason, *Ccp1*-KO MEFs were employed for these analyses. The animal source of these cells is considered equivalent to PCD mice since they also lack mRNA expression of *Ccp1* [10, 14]. All the procedures were standardized in these PCD-like cells at Joseph Fourier University to ensure the feasibility and reliability of these experiments. MEFs from the brains of 13.5-day-old WT and *Ccp1*-KO mouse embryos were isolated following standard procedures as previously described [14, 45, 46]. Briefly, MEFs were cultured in Dulbecco's modified Eagle's medium (DMEM; Life Technologies, Gibco) supplemented with 10% fetal bovine serum (FBS) until they reached 80% confluence. Afterwards, to visualize microtubules, MEFs were transfected with different plasmids; Nucleofector™ Kits for MEFs (Amaxa Biosystems) were used to transfect cells with GFP-EB3 to visualize microtubule plus-ends in green (provided by N. Galjart, Erasmus Medical Center, Rotterdam, The Netherlands) and m-cherry α-tubulin to visualize the entire microtubule structure in red (provided by F. Saudou, Curie Institute, Paris, France) as previously described [14].

Cell Culture Treatments

Cells were divided into experimental groups (n = 3 embryos per group) on the basis of genotype (WT or PCD) and the concentration of OEA administered (0, 0.1, 0.5, or 1.0 μM) based on previous works [26]. OEA was dissolved in 100% DMSO and stored at − 80°C. On the day of the experiment, OEA was diluted in culture medium (DMEM + 10% FBS) at the appropriate concentration and added to the cells. Control (untreated) cells from WT and PCD animals were also cultured with the same concentration of DMSO to avoid possible confounding effects.

Analysis of Microtubule Structure and Dynamics

Microtubule dynamics were analyzed using images from time-lapse videos of GFP-EB3 staining and plusTipTracker software [47]. Time-lapse videos of transfected MEFs were captured with an inverted microscope (Axio-vert 200 M; Carl Zeiss, Inc., Oberkochen, Germany) and a × 100 NA 1.3 Plan-Neofluar oil objective that was controlled with MetaMorph software (MDS Analytical Technologies, CA, USA). Images were captured with a charge-coupled device camera (CoolSNAP HQ; Roper Scientific, Vianen, The Netherlands) every 3 s for 5 min. The parameters that were analyzed were growth and shrinking speed; growth and shrinking mean length; percentage of time in pause, growing, and shrinking; frequency of catastrophes (changes from growing to shrinking); frequency of rescues (changes from shrinking to growing); microtubule curvature (statics); and microtubule trajectory curvature (movement) based on previous studies [14, 46, 47]. Briefly, parameters related to growth and shrinking processes were analyzed using the complete sequence images time-lapse videos of GFP-EB3 (labels microtubule plus-ends) staining, whereas for static microtubule curvature analysis, the first image of each video time-lapse video of m-cherry α-tubulin (labels the entire microtubule) staining was employed. Additionally, for GFP-EB3 labeling, we obtained the maximum projection of the entire time-lapse video, allowing us to reconstruct the movement trajectory curvatures of the microtubule plus-ends as previously described [14].

Statistical Analysis

The results are expressed as the means ± standard errors of the mean (SEMs). Homoscedasticity and normality were checked prior to all of the statistical analyses (Kolmogorov–Smirnov's and Levene's tests). Due to the complexity and variability of the conditions analyzed in the *in vivo* and *in vitro* experiments and to facilitate comprehension, each statistical test and the variables compared are provided with the results of each corresponding experiment. All analyses were performed using SPSS software for Windows V25 (IBM, NY, USA).

Results

Expression of Endocannabinoid Receptors in PCD Mice

Before starting the *in vivo* OEA experiment, we analyzed the expression of components of the endocannabinoid system throughout postnatal cerebellar development, focusing primarily on PPARα since it is considered the main target through OEA exerts its actions [35]. On the one hand, PPARα was detected and quantitatively analyzed in the three cerebellar layers of the cerebellum in both genotypes at all analyzed (Fig. 2a–c). However, Student's *t* test showed that the percentage of Purkinje cells expressing PPARα was slightly lower in the mutant animals than in the WT animals from P15 onward (Fig. 2d; P15, $p < 0.05$; P17, $p < 0.05$; P22, $p < 0.05$). On the other hand, due to the diffuse expression and distribution of the canonical cannabinoid receptors CB1 and CB2 in the cerebellum, the analysis of their expression was qualitatively performed. CB1 receptors were expressed in the molecular layer from P7 onwards and in the basket cells of "Pinceaux formation" from P17 onwards. However, no qualitative differences in CB1 expression were detected between genotypes at any of the ages analyzed (Fig. 2c). By contrast, the expression of CB2 seemed to increase in the PCD mice during the neurodegenerative process (from P22) and colocalized with the apical radial processes of the Bergmann glial cells (Supplementary Fig. 1). Anyway, the finding that PPARα is expressed in the cerebellum led us to believe that OEA may exert a neuroprotective effect on Purkinje cells in PCD mice *in vivo*.

OEA Administration Increases PPARα Expression in PCD Mice

After demonstrating that PPARα is expressed during postnatal cerebellar development, we assessed the influence of OEA administration on the expression of PPARα in PCD mice. One-way ANOVA followed by Dunnett's post hoc test revealed an increase in the percentage of Purkinje cells expressing PPARα in PCD mice when OEA was administered at doses of 5 and 10 mg/kg, independent of the schedule of administration (Fig. 2e, Supplementary Fig. 2; 5 mg/kg, $p < 0.05$; 10 mg/kg, $p < 0.01$).

Fig. 2 Expression of the PPARα endocannabinoid receptor in the cerebellum. (**a**, **b**) Sagittal section of the vermis of a WT mouse (**a**) and confocal image with tridimensional projection (**b**) showing the co-localization of PPARα (green) in Purkinje cells (Cb28k, red) at P30. (**c**) Micrographs showing the expression of the PPARα (red), CB1 receptor (green), and Purkinje cells (Cb28k, blue) in WT and PCD mice throughout the postnatal cerebellar development (P7, P15, P17, P22, P30); PPARα expression can be observed in the three cerebellar layers at all postnatal ages. The CB1 receptor is expressed in the molecular layer from P7 onwards. In addition, from P15 onward, the CB1 receptor begins to be expressed around Purkinje cell somata (Cb28k positive), leading to the "Pinceaux formation." (**d**) Quantification of the percentage of Purkinje cells expressing PPARα at different time points of the postnatal cerebellar development; note that this value is lower in PCD mice than in WT from P15 to P22. (**e**) Quantification of the percentage of PCD's Purkinje cells expressing PPARα at P30 after different OEA dosages; OEA administration leads to an increase in the number of Purkinje cells expressing PPARα in the three different treatments at doses of 5 and 10 mg/kg. Data are represented as mean ± SEM; $n = 4$ each experimental group; Student's *t* test for (**d**); one-way ANOVA followed by Dunnett's post hoc test for (**e**); $^{*}p < 0.05$; $^{**}p < 0.01$

OEA Prevents Alterations in the Morphology of Purkinje Cells

We then analyzed the effect of OEA administration on progressive morphological alterations in PCD Purkinje cells. Our first objective was to determine the effectiveness of different OEA doses (1, 5, or 10 mg/kg) and administration schedules (chronically from P7–P21 or acutely at P14 or P16) on the maintenance of Purkinje cell morphology (Fig. 3a–h). One-way ANOVA followed by Dunnett's post hoc test was performed to compare each dose and administration schedule *vs.* control treatment. Analysis of the data at P30 showed that chronic and acute administration of both 5 and 10 mg/kg OEA prior to the preneurodegenerative stage ameliorated morphological alterations in Purkinje cells (Fig. 3i–l). In contrast, when OEA was administered at P16, only the highest dose, 10 mg/kg, was effective in alleviating some of the morphological changes (Fig. 3i–l).

Then, we carried out a second set of experiments to improve further the therapeutic effect of OEA *in vivo*. Based on the previous results and to reduce animal suffering, we administered a single injection of the most effective dose of OEA (10 mg/kg) prior to preneurodegeneration. We compared the effect of OEA administration at three time points (P14, P12, P10, i.e., one, three or five days before the onset of neurodegeneration in PCD mice, respectively) by one-way ANOVA followed by Bonferroni's post hoc test (Fig. 4). The results of this analysis showed that acute administration at

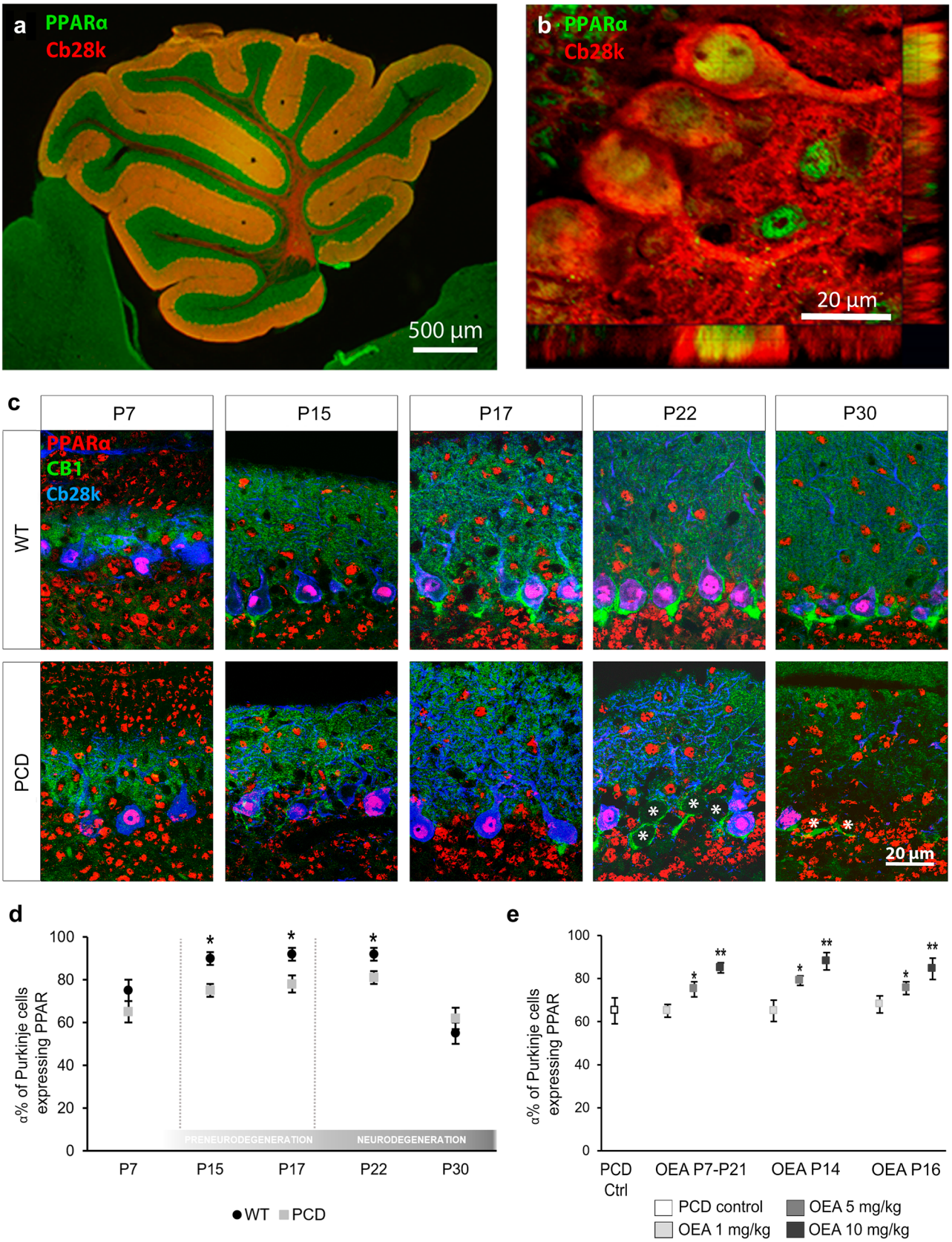
a
PPARα
Cb28k
500 µm
b
PPARα
Cb28k
20 µm
c
P7
P15
P17
P22
P30
WT
PCD
PPARα
CB1
Cb28k
20 µm
d
a% of Purkinje cells expressing PPAR
PRENEURODEGENERATION
NEURODEGENERATION
P7
P15
P17
P22
P30
WT
PCD
e
a% of Purkinje cells expressing PPAR
PCD Ctrl
OEA P7-P21
OEA P14
OEA P16
PCD control
OEA 1 mg/kg
OEA 5 mg/kg
OEA 10 mg/kg

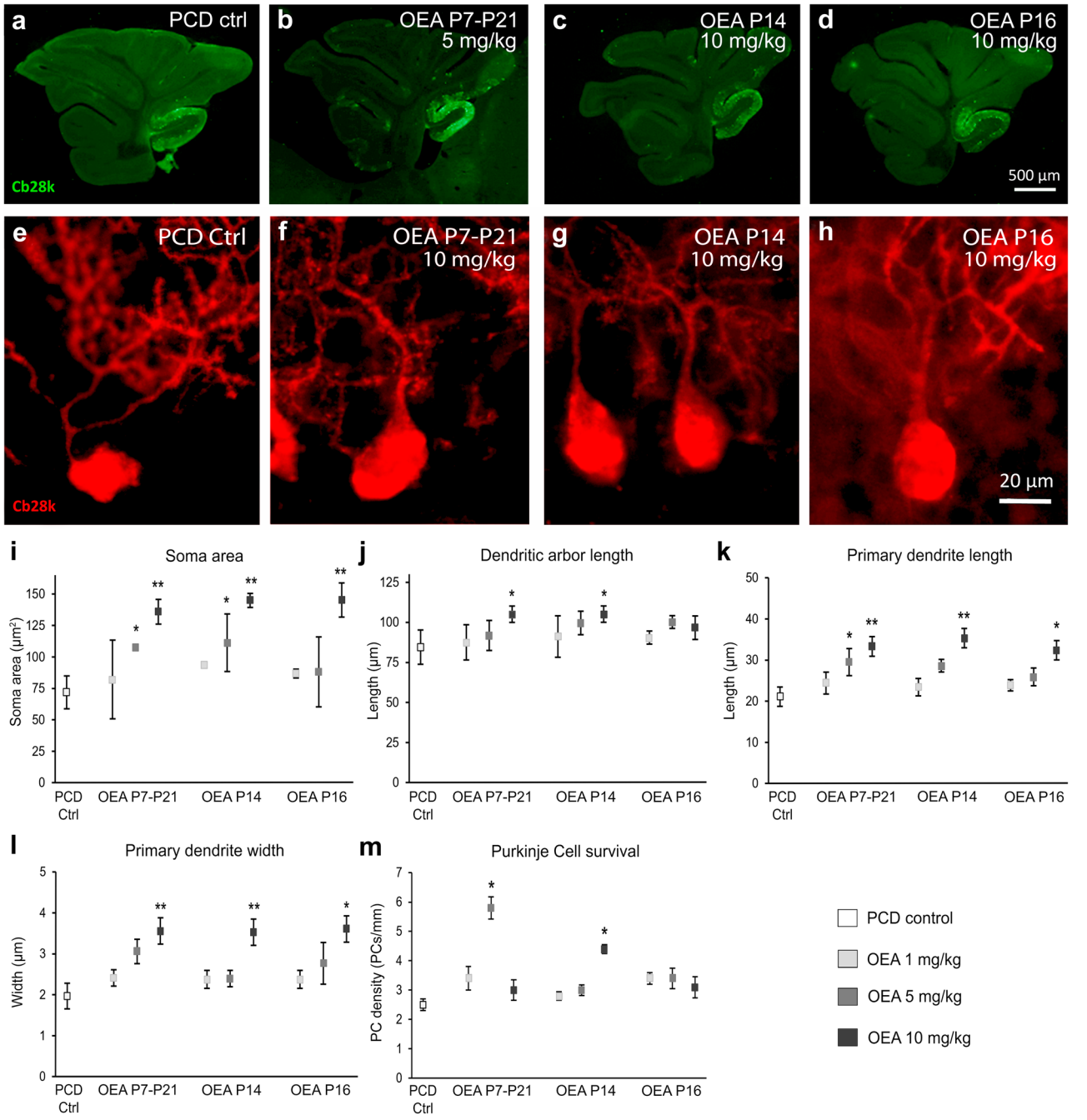

Fig. 3 *In vivo* effect of different OEA dosages on the morphology and survival of the Purkinje cells of the PCD mouse analyzed at P30 (first set of experiments). (**a**–**d**) Micrographs of PCD cerebellar vermis slices labeled with calbindin (Cb28k, green) after different OEA treatments: control (**a**), chronic administration from P7 to P21 of 5 mg/kg (**b**), acute administration of 10 mg/kg at P14 (**c**), acute administration of 10 mg/kg at P16 (**d**). (**e**–**h**) Micrographs of Purkinje cells labeled with calbindin (Cb28k; red) in PCD animals treated with different dosages of OEA: control (**e**), chronic administration from P7 to P21 of 10 mg/kg (**f**), acute administration of 10 mg/kg at P14 (**g**), acute administration of 10 mg/kg at P16 (**h**). (**i**–**l**) Quantification of the OEA effect on different morphological parameters of PCD Purkinje cells; note that the chronic and acute administration at P14 have a stronger neuroprotective effect than the acute administration at P16 in all the parameters evaluated. (**m**) Quantification of PCD Purkinje cell survival at different OEA dosages; note that both chronic administration at a dose of 5 mg/kg and acute administration at P14 at a dose of 10 mg/kg prevented Purkinje cell death. Data are represented as mean ± SEM; $n = 4$ each experimental group; one-way ANOVA followed by Dunnett's post hoc test for (**i-m**) * $p < 0.05$; ** $p < 0.01$

the three time points prevented morphological alterations at P30 (Fig. 4i–l). Furthermore, this neuroprotective effect followed an inverted U-shaped time-response curve, with acute administration at P12 being the most effective administration time point for preventing Purkinje cell morphological alterations, as the morphological parameters reached values similar to those of WT animals (Fig. 4i–l). Next, we decided to determine whether this neuroprotective effect of OEA administered at P12 was maintained over time. However, the results at P40 showed that the values of only two of the parameters analyzed (soma area and primary dendrite length) were maintained (Supplementary Fig. 3).

OEA Administration Decreases Purkinje Cell Death

One-way ANOVA followed by Dunnett's post hoc test was performed to compare the effect of different OEA doses used in the first set of experiments on Purkinje cell survival. The results showed that chronic administration of OEA at a dose of 5 mg/kg ($p < 0.05$) but not 1 or 10 mg/kg from P7-P21 had a preventive effect on Purkinje cell death (U-shaped response). OEA administration at P14 also ameliorated this degeneration, but only at a dose of 10 mg/kg ($p < 0.05$). In contrast, when OEA was administered at P16, that is, after preneurodegeneration had already started, the treatment had no effect on Purkinje cell death (Fig. 3m). Thus, similar to the findings related to Purkinje cell morphology, OEA seems to increase Purkinje cell survival only when it is administered prior to the onset of preneurodegeneration. As before, we compared the effect of acute preventive treatment at P14, P12, and P10 on Purkinje cell survival by performing one-way ANOVA followed by Bonferroni's post hoc test. The results confirmed that acute administration of OEA (10 mg/kg) reduced Purkinje cell degeneration when administered prior to the onset of preneurodegeneration at either P12 ($p < 0.01$) or P14 ($p < 0.05$). This effect also followed an inverted U-shaped time-response curve, with OEA administration at P12 being the most effective treatment (Fig. 4m; $p < 0.01$). OEA administration at P10 had no effect on Purkinje cell density. Moreover, the number of Purkinje cells in animals treated at P10 seemed to be even lower than that in untreated PCD mice, probably due to the deleterious effects of OEA at very early stages (Fig. 4m). Indeed, the weight of the PCD animals treated at P10 was significantly lower than that of the rest of the PCD animals (Supplementary Table 1).

Effect of OEA on Motor Coordination

Once both the neuroprotective properties of OEA were demonstrated histologically and the most effective therapeutic time window was identified, we wondered whether the cellular neuroprotective effects of OEA could be translated into an improvement in behavioral impairments in PCD mice. To answer this question and to reduce the number of animals employed in the study, we analyzed the effect of only the most effective OEA treatment regimen (10 mg/kg, i.p. at P12) on the motor, cognitive, and social behavior of PCD mice throughout the entire neurodegenerative process (at P15, P17, P22, P30, and P40). First, to study motor coordination, we subjected mice in the three experimental groups (WT mice, PCD mice and PCD mice treated at P12) to the *rotarod* test (Fig. 5a). One-way repeated-measures ANOVA results revealed that *rotarod* data test violated sphericity (p Mauchly's test < 0.01). They exhibited statistically significant differences within the 'day of testing' factor ($p < 0.01$) and the 'experimental group' factor ($p < 0.01$) separately; and in the interaction between both factors 'experimental group' * 'day of testing' ($p < 0.01$), for the four criteria of the multivariate analysis (Pillai's trace, Wilks' Lambda, Hotelling's trace and Roy's largest root). Graphic representation of the *rotarod* test data showed that the general motor performance of the three experimental groups diverged over time (which can explain the interaction between factors, see "Discussion"), with the most significant differences being between the WT and PCD mice (Fig. 5b). The performance of the WT mice in the *rotarod* test gradually improved until P30 and then stabilized, probably due to learning (Fig. 5b). However, treated PCD mice showed similar behavior as WT mice until P22 but then gradually exhibited motor behavior that was more similar to that of untreated PCD animals (Fig. 5b). To evaluate further the possible differences between the three experimental groups within each day of testing, we performed one-way ANOVA followed by Bonferroni's post hoc test on each day of *rotarod* testing. These results revealed that the motor behavior of WT, untreated PCD and treated PCD mice was similar at P15 ($p > 0.05$), but differed from each other from P17 onwards (Fig. 5b; P17, $p < 0.01$; P22, $p < 0.01$; P30, $p < 0.01$; P40, $p < 0.01$). First, the motor coordination of PCD mice (both untreated and treated) was affected compared to that of WT animals since the beginning of preneurodegeneration except for P15 (untreated PCD mice: $p < 0.01$ for P17, P22, P30, and P40; treated PCD mice: $p < 0.01$ for P17, P22, P30 and P40). However, PCD animals treated with OEA showed an improvement in the performance of the *rotarod* test at P22 and P30 compared to untreated PCD mice (Fig. 5b; P22, $p < 0.05$; P30, $p < 0.05$). Unfortunately, this amelioration was not detected at P40 when motor behavior of both treated and untreated PCD were similar and no differences were detected between these two experimental groups ($p > 0.05$). These finding indicates that although OEA treatment did not completely restore the normal motor coordination of PCD mice, it contributed to improving it since the motor behavior of

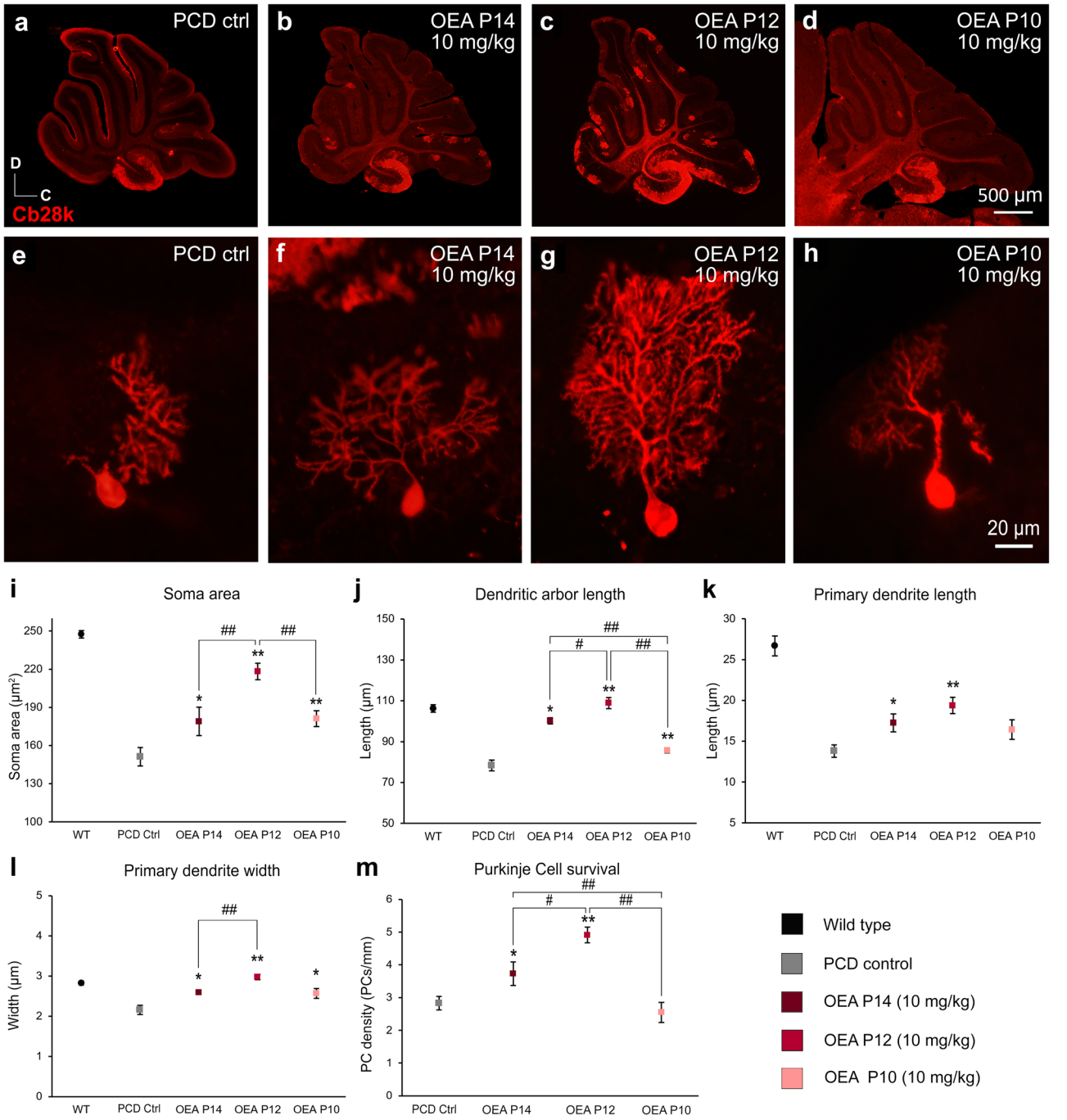

Fig. 4 *In vivo* effect of different acute administration of OEA on the morphology and survival of the Purkinje cells of the PCD mouse analyzed at P30 (second set of experiments). (**a**–**d**) Micrographs of PCD cerebellar vermis slices labeled with calbindin (Cb28k, red) at different OEA acute administrations at a dose of 10 mg/kg: control (**a**), at P14 (**b**), at P12 (**c**), and at P10 (**d**); an increase in the Purkinje cell density can be qualitatively observed when OEA is administered at P12. (**e**–**h**) Micrographs of Purkinje cells labeled with calbindin (Cb28k; red) in PCD animals administered with OEA (10 mg/kg) at P14 (**f**), P12 (**g**), and P10 (**h**); a notable improvement in the Purkinje cell arborization can be qualitatively observed when OEA is administered at P12. (**i**–**l**) Quantification of the effect of OEA on Purkinje cells morphology; note that the neuroprotective effect of OEA administered acutely follows an inverted U-shaped time-response curve, with acute administration of OEA at P12 being the most effective treatment for stabilizing Purkinje cell morphology, as the morphological parameters reached values similar to those of WT animals. (**m**) Quantification of the effect of OEA on Purkinje cell survival. Data are represented as mean ± SEM; $n = 7$ each experimental group; one-way ANOVA followed by Bonferroni's post hoc test for (**i**–**m**); $*p < 0.05$, $**p < 0.01$ for differences between experimental group and control group (PCD without treatment); $\#p < 0.05$, $\#\#p < 0.01$ for differences between the different OEA treatments. Data from WT animals has been used only as a reference, not to compare

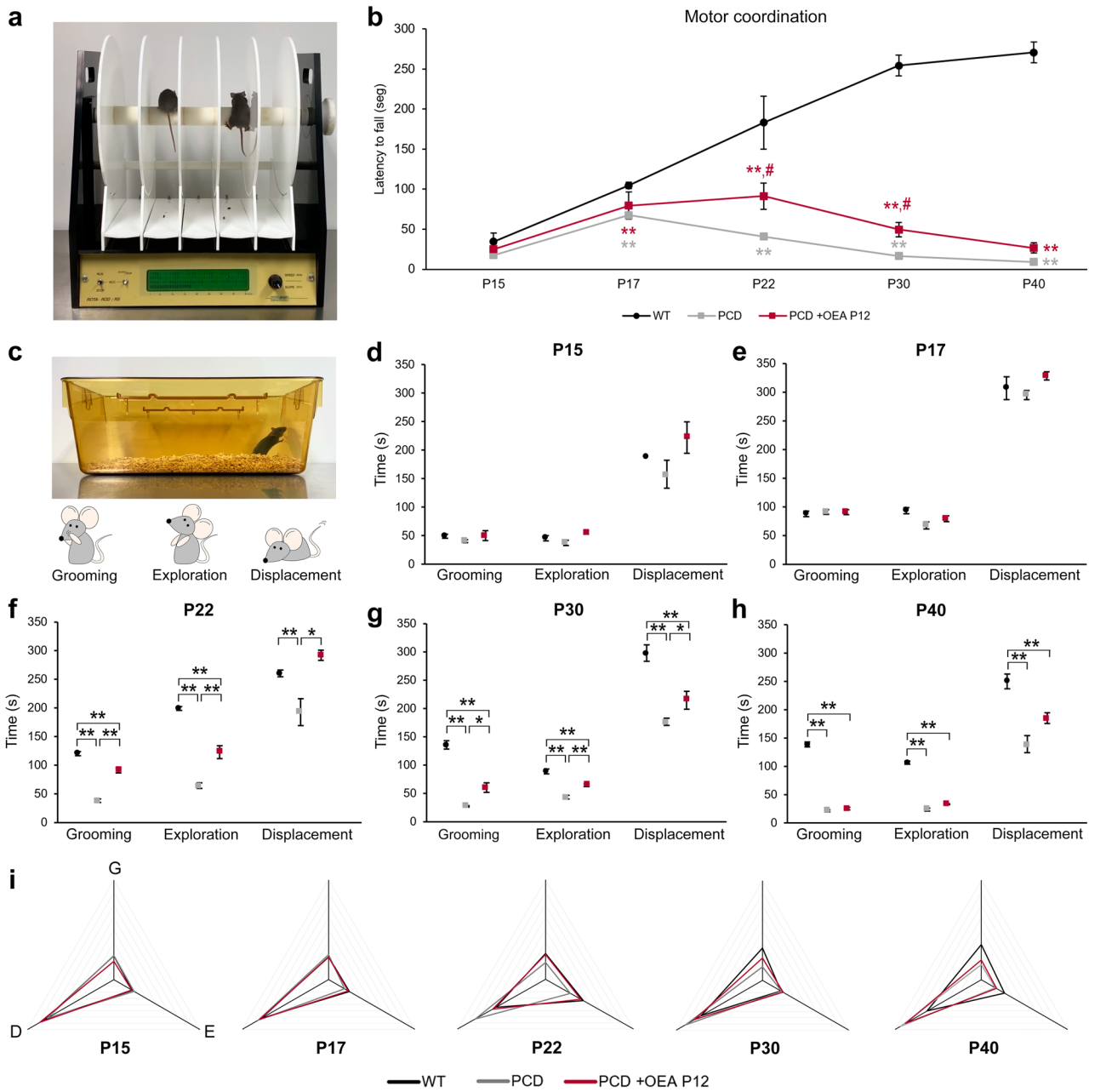

Fig. 5 Analysis of the effect of OEA on motor coordination and general behavior along cerebellar degeneration. (**a**, **b**) Representation and quantification of the *rotarod* test at different ages for WT, PCD, and treated PCD mice; note that both treated and untreated PCD motor behavior was impaired from P17 onward; however, OEA treatment improve the *rotarod* motor task of PCD animals at P22 and P30 although it did not completely restore it. In this graph, $^{**}p < 0.01$ for differences between WT and PCD experimental groups; $\#p < 0.05$, for differences between PCD experimental groups (i.e., treated and untreated PCD). (**c**–**h**) Representation and quantification of the parameters analyzed in the home-cage behavior analysis at different ages; note that the general behavior is similar for the three experimental groups until P17. From P22 onward treated PCD behavior is always halfway between WT and nontreated PCD until P40, at which time no OEA effect was observed. (**i**) Profile representation of the percentage of time displacing, grooming, and rearing with respect to the total amount of time active; note that WT and treated PCD behave similarly at all ages analyzed until P30. Data are represented as mean ± SEM; $n = 8$–9 each experimental group; one-way ANOVA followed by Bonferroni's post hoc test for (**b**), (**d**–**h**); $^{*}p < 0.05$; $^{**}p < 0.01$

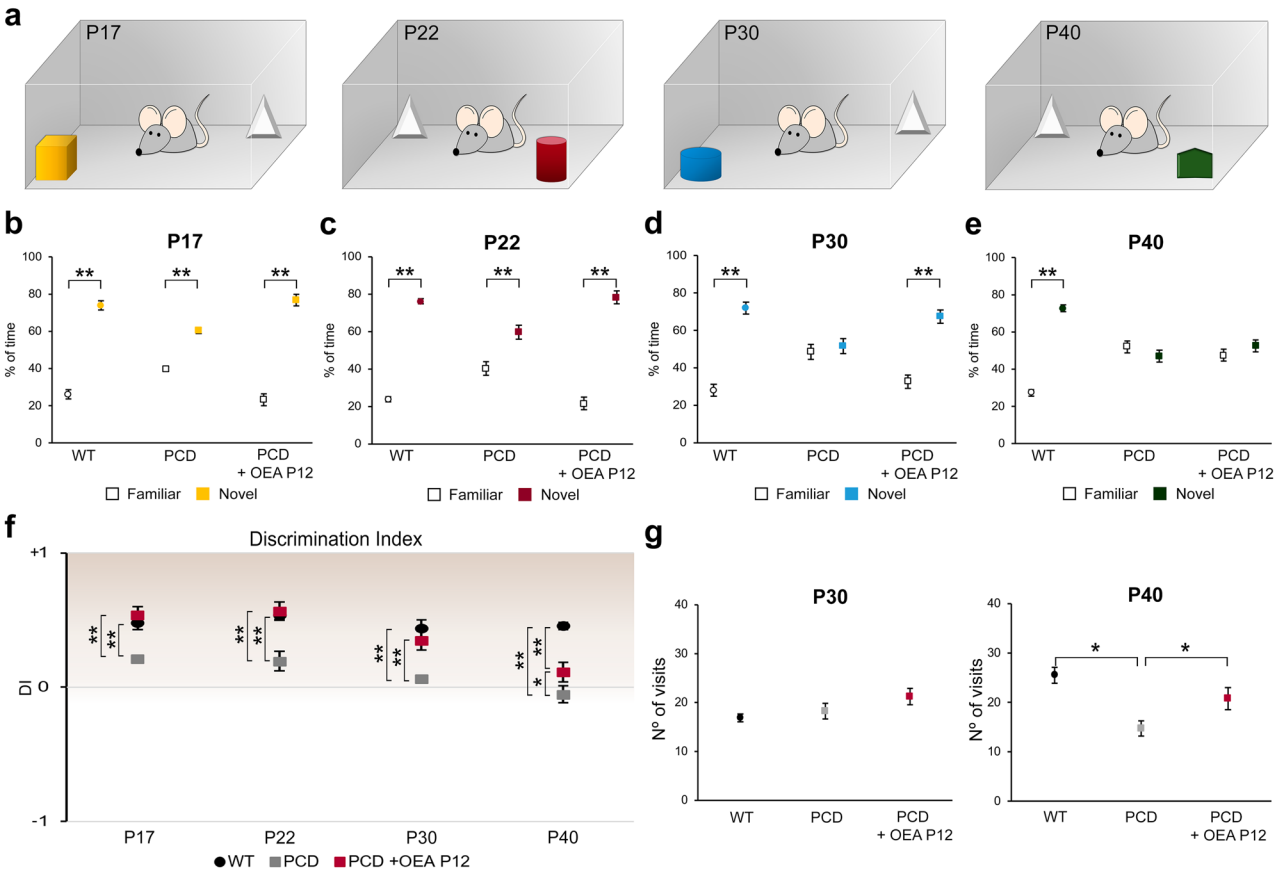

Fig. 6 Analysis of the effect of OEA on recognition memory along cerebellar degeneration. (**a**) Schematic representation of the NOR test and the objects employed. (**b**–**e**) Analyses of the percentage of time exploring familiar and novel objects at different ages for WT, PCD, and treated PCD animals; the preference for new objects is maintained in treated PCD mice until P30. (**f**) Chart showing the discrimination index at different ages for WT, PCD, and treated PCD mice; note that this index is similar in WT and treated PCD until P30, always resulting in a positive score greater than zero, which means there is a preference for novel objects. (**g**) Quantification of the number of visits to both objects at P30 and P40; no differences were observed at P30 while at P40 a decrease in the number of visits was detected in nontreated PCD. Data are represented as mean ± SEM; $n = 8$–9 each experimental group; Student's t test for (**b**–**e**); one-way ANOVA followed by Bonferroni's post hoc test for (**f**, **g**); $^{*}p < 0.05$; $^{**}p < 0.01$

treated mice was midway between that of WT and untreated PCD animals at P22 and P30.

OEA Treatment Normalizes the General Behavior of PCD Mice

Second, for the home-cage behavior test (Fig. 5c), one-way ANOVA followed by Bonferroni's post hoc test was performed for each parameter measured. Overall, the three experimental groups showed similar results with respect to grooming time, exploratory behavior and displacement at P15 and P17 (Fig. 5d, e). Conversely, from P22 onward, these three variables were different between the WT and PCD animals (Fig. 5f–h). The grooming time, exploratory behavior, and displacement of the treated PCD mice were increased compared to those of the untreated PCD animals at P22 and P30 (grooming P22, $p < 0.01$; grooming P30, $p < 0.05$; exploration P22, $p < 0.01$; exploration P30, $p < 0.01$; displacement P22, $p < 0.05$; displacement P30, $p < 0.05$; Fig. 5f, g), being more similar to the values of the WT mice. However, this effect was not maintained at P40, at which time no differences were detected between the groups of PCD mice (Fig. 5h). To allow better visual comprehension, in Fig. 5i, the percentages of time dedicated to grooming, exploration and displacement with respect to total activity time are depicted as a triangle for each experimental group, with each of the vertices representing on the analyzed parameters (grooming, exploration and displacement). Briefly, the general behavior triangles of the WT mice and both groups of PCD mice were similar at P15 and P17. However, at P22, the triangle of the untreated PCD mice started to differ, while that of the treated PCD mice remained identical to that of the WT mice. Finally, at P30 and P40, the triangle of the treated PCD mice was positioned midway

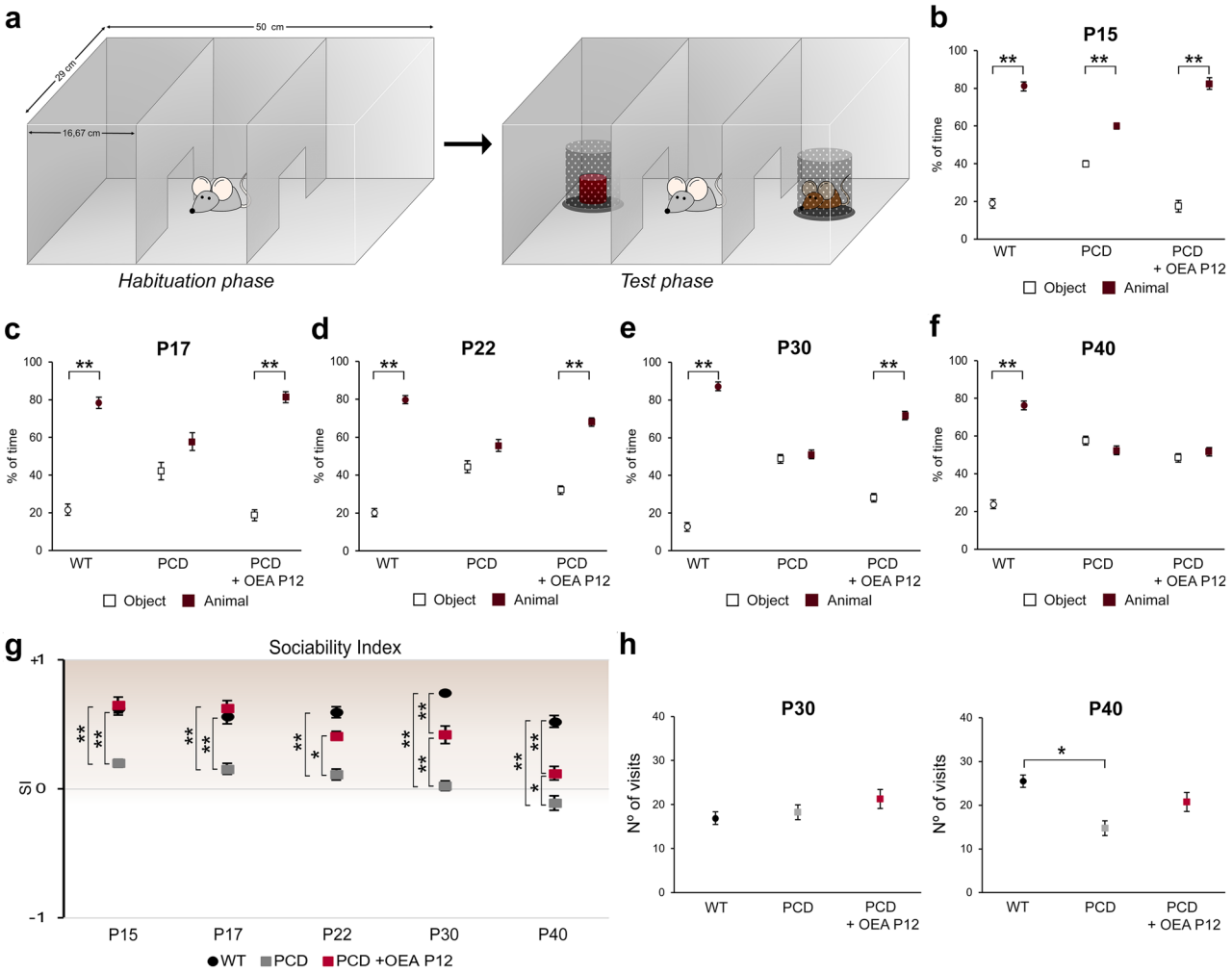

Fig. 7 Analysis of the effect of OEA on social behavior along cerebellar degeneration. (**a**) Schematic representation of the three-chambered social preference test. (**b–f**) Quantification of the percentage of time spent exploring the chamber, containing either an intruder or an object, by WT, PCD, and treated PCD at different ages; note that the normal social behavior was impaired in nontreated PCD mice from P17 onward, whereas treated PCD animals maintained a normal social pattern until P30. (**g**) Chart showing the sociability index at different ages for WT, PCD, and treated PCD animals; similar values were observed in WT and treated PCD mice until P30, at which time the treated PCD subjects showed an intermediate score between WT and nontreated PCD mice. (**h**) Quantification of the number of visits to both objects at P30 and P40; a decrease in the number of visits was detected in nontreated PCD mice at P40. Data are represented as mean ± SEM; $n = 8–9$ each experimental group; Student's t test for (**b–f**); one-way ANOVA followed by Bonferroni's post hoc test for (**g**, **h**); $^{*}p < 0.05$; $^{**}p < 0.01$

between that of the WT and untreated PCD mice, which was consistent with the *rotarod* results and histological analyses.

OEA Administration Prevents Memory Impairments Until P30

Long-term memory recognition was assessed by the NOR test. Comparison of the percentage of time spent exploring the novel and familiar objects by each experimental and age group by Student's t test (Fig. 6a) showed that WT mice spent a greater percentage of time exploring the novel object than the familiar object at all analyzed ages (Fig. 6b–e; P17, $p < 0.01$; P22, $p < 0.01$; P30, $p < 0.01$; P40, $p < 0.01$). PCD mice showed the same behavior at P17 ($p < 0.01$) and P22 ($p < 0.01$), but at P30 and P40, no differences were detected between the time exploring the novel and familiar objects. The treated PCD mice spent a greater percentage of time exploring the new object than the familiar object until P30, indicating that OEA administered at P12 preserved long-term memory recognition (Fig. 6b–e; P17, $p < 0.01$; P22, $p < 0.01$; P30, $p < 0.01$). However, at P40, no differences were detected in this group, which is consistent with the histological results and the results of the previous behavioral tests (Fig. 6e and Supplementary Fig. 3).

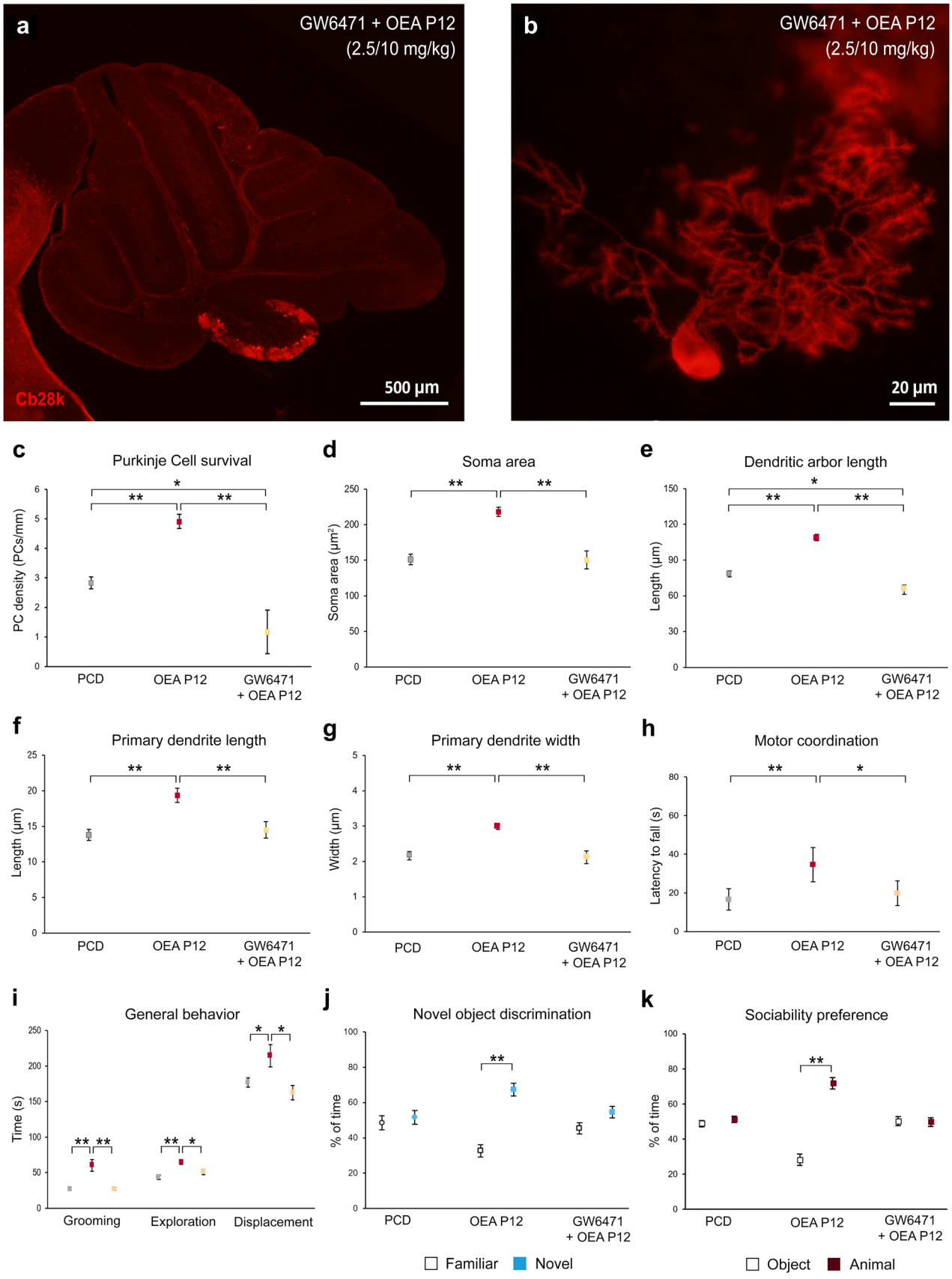
a
GW6471 + OEA P12
(2.5/10 mg/kg)
Cb28k
500 µm
b
GW6471 + OEA P12
(2.5/10 mg/kg)
20 µm
c
Purkinje Cell survival
PC density (PCs/mm)
PCD
OEA P12
GW6471 + OEA P12
d
Soma area
Soma area (µm²)
e
Dendritic arbor length
Length (µm)
f
Primary dendrite length
Length (µm)
g
Primary dendrite width
Width (µm)
h
Motor coordination
Latency to fall (s)
i
General behavior
Time (s)
Grooming
Exploration
Displacement
j
Novel object discrimination
% of time
Familiar
Novel
k
Sociability preference
% of time
Object
Animal

◂**Fig. 8** The neuroprotective effect of OEA treatment is mediated by PPARα receptors.(**a**, **b**) Micrographs of cerebellar vermis (**a**) and a Purkinje cell (**b**) labeled with calbindin (Cb28k, red) of a mouse treated with the PPARα antagonist GW6471 (2.5 mg/kg, i.p.) and OEA (10 mg/kg, i.p. P12). (**c**–**g**) Histological quantification of the effect of GW6471 + OEA at P12 on the Purkinje cell survival (**c**) and on Purkinje cell morphology (**d**–**g**); note that the neuroprotective effect of OEA observed was abolished when PPARα receptor was blocked by GW6471. (**h**–**k**) Motor, cognitive and social analysis of PCD mice treated with GW6471 + OEA at P12; note that animals pretreated with the antagonist of PPARα showed the same behavior as untreated PCD mice, suggesting that OEA exerts its neuroprotective effect via a PPARα-dependent pathway. Both histological and behavioral analyses were performed at P30. Data are represented as mean ± SEM; $n = 5$ each experimental group; one-way ANOVA followed by Bonferroni's post hoc test for (**c**–**i**); Student's t test for (**j**, **k**); $^{*}p < 0.05$; $^{**}p < 0.01$

In parallel, one-way ANOVA followed by Bonferroni's post hoc test was performed to analyze the DI. The results presented in Fig. 6f show no differences between WT and treated PCD animals from P17 to P30; both groups of animals had positive values, indicating that more time was spent examining the novel object. Although a positive DI was maintained for the treated PCD mice at P40, it was between the DIs of WT and untreated PCD mice. Finally, the DIs of untreated PCD mice were positive until P30, when they became negative, indicating that the mice exhibited no preference toward the novel object.

The number of visits to both objects was analyzed at all ages to avoid possible biases derived from motor alterations in PCD mice. ANOVA followed by Bonferroni's post hoc test did not reveal differences in the number of visits between the experimental groups at P17, P20 and P30. However, at P40, the number of times that PCD mice visited both objects was lower than the number of times WT or treated PCD animals visited the objects (Fig. 6g). This finding showed that ataxia affected the ability of PCD mice to perform this task at P40, which may have interfered with the results obtained at this age (see "Discussion").

Normal Social Behavior Is Maintained After OEA Administration Until P30

Social behavior was assessed by the three-chambered social preference test. The percentage of time interacting spent with a hidden animal or object was compared by each experimental and age group using Student's t test. The results of this test (Fig. 7a) showed a preference for social contact in WT animals at all ages (Fig. 7b–f; P15, $p < 0.01$; P17, $p < 0.01$; P22, $p < 0.01$; P30, $p < 0.01$; P40, $p < 0.01$), while PCD mice showed a nonsocial preference from P17 onward, spending the same percentage of time exploring the compartment containing the mouse as the one containing the object (Fig. 7b–f; P17, $p > 0.05$; P22, $p > 0.05$; P30, $p > 0.05$; P40, $p > 0.05$). Conversely, treated PCD mice spent a larger percentage of time exploring the chamber containing the mouse than the one containing the object until P30, indicating recovery of normal social behavior up to this age (Fig. 7b–e; P15, $p < 0.01$; P17, $p < 0.01$; P22, $p < 0.01$; P30, $p < 0.01$). Unfortunately, this effect was not observed at P40, at which point treated PCD mice and untreated PCD mice spent the same percentage of time exploring both compartments (Fig. 7f; $p > 0.05$).

One-way ANOVA followed by Bonferroni's post hoc test was performed to analyze the SI. The results presented in Fig. 7g show that the SIs of WT mice remained positive at all ages analyzed. Likewise, the treated PCD mice had similar SIs as WT animals until P30, at which point the SIs of treated PCD mice remained positive but diverged from the SIs of WT mice. Finally, the SIs of PCD mice were close to 0 or negative at all ages analyzed, indicating that these mice preferred to behave in a nonsocial manner.

The number of visits to both compartments was also analyzed at all ages. ANOVA followed by Bonferroni's post hoc test revealed differences only at P40, at which point the total number of visits made by the PCD animals was lower than that made by the WT and treated PCD mice (Fig. 7h). This result may have distorted the results of the three-chambered test at P40.

The *In vivo* Neuroprotective Effects of OEA Are Mediated by PPARα

To test whether the endocannabinoid PPARα mediates the neuroprotective effects of OEA observed in PCD mice at both the histological and behavioral levels, the PPARα antagonist GW6471 (2.5 mg/kg b.w., i.p.) was injected into an additional group of mice 15 min before OEA treatment (10 mg/kg b.w., i.p.). Histological and behavioral experiments were performed as described above. The results of histological analyses at P30 (Fig. 8) showed that the administration of the PPARα antagonist fully blocked the neuroprotective effect of OEA on all the parameters related to Purkinje cell morphology and survival (Fig. 8a–g; $p < 0.01$ for all histological parameters). Regarding Purkinje cell survival, a lower density of Purkinje cells was observed in animals pretreated with GW6471 than in untreated PCD mice (Fig. 8c; $p < 0.01$). Therefore, the PPARα antagonist not only abolished the neuroprotective effect of OEA on Purkinje cell survival but also increased Purkinje cell death. In addition, the improvements in motor, cognitive and social behavior observed in treated PCD mice were fully suppressed when PPARα was blocked prior to OEA treatment (Fig. 8h–k). These results indicate that PPARα is the main receptor involved in the actions of OEA in PCD mice.

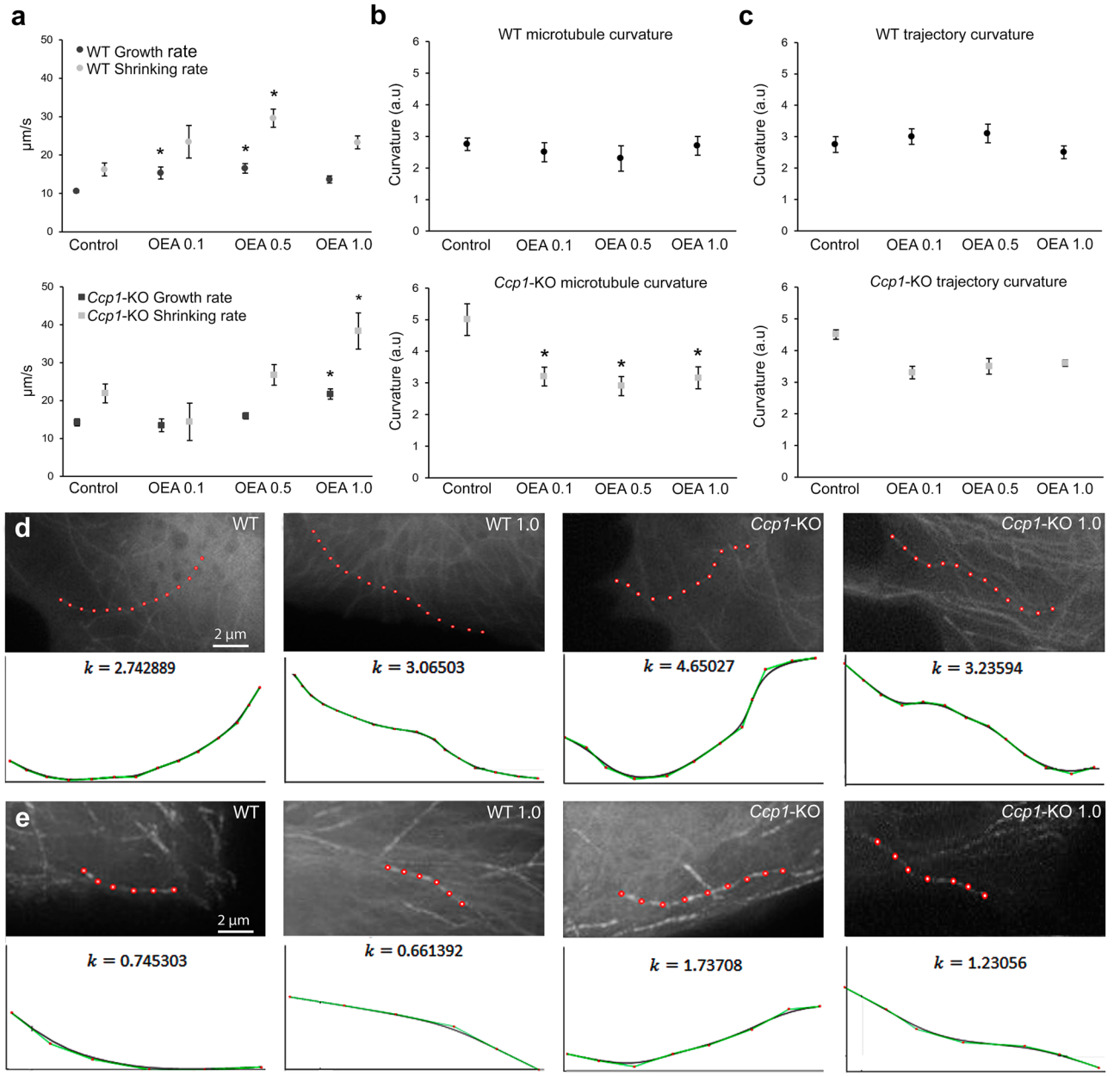

Fig. 9 *In vitro* effect of OEA on WT and *Ccp1*-KO microtubule dynamics of MEFs.(**a**) Analyses of WT and *Ccp1*-KO microtubule growth and shrinking rates; OEA administration affects both parameters and experimental groups in a dose-dependent manner, although a higher OEA concentration is required in *Ccp1*-KO cells. (**b**) Analyses of WT and *Ccp1*-KO static microtubule curvature; OEA administration decreased *Ccp1*-KO microtubule curvature but did not affect WT curvature. (**c**) Analyses of WT and *Ccp1*-KO microtubule trajectory curvature; OEA did not affect trajectory curvature in any of the two genotypes. (**d**, **e**) Examples of WT and *Ccp1*-KO microtubule curvature (**d**) and trajectory (**e**) in control and OEA-administered cells (1.0 μM) and the corresponding graphical representation. Data are represented as mean ± SEM; $n = 3$ embryos per experimental group; a.u. = arbitrary units; one-way ANOVA followed by Dunnett's post hoc test for (**a**–**c**); $^*p < 0.05$

OEA Increases Microtubule Dynamics and Restores Microtubule Shape *In vitro*

After demonstrating that OEA exerts its neuroprotective effects *in vivo* in PCD mice at both the histological and behavioral levels through PPARα and given that excess microtubule polyglutamylation in mutant cells triggers alterations in both the dynamics and structure of microtubules [10, 13, 14], we wondered whether the molecular effect of OEA could be related to these microtubule characteristics. To answer this question, we employed an additional *in vitro* MEF model that allowed us to visualize

individual microtubules since these analyses cannot be properly performed *in vivo* due to the structural complexity and highly branched dendritic trees of Purkinje neurons. One-way ANOVA followed by Dunnett's post hoc test was employed to compare the effect of the different OEA doses *vs.* control treatment (untreated WT and untreated *Ccp1*-KO cells) separately for each genotype. The results showed that OEA modified the dynamics and structure of microtubules in cells of both genotypes (Fig. 9). Regarding microtubule dynamics, OEA increased the growth and shrinkage rates of both WT ($p < 0.05$) and *Ccp1*-KO ($p < 0.05$) microtubules (Fig. 9a). However, the OEA concentration required for a significant effect was higher in *Ccp1*-KO cells (1.0 µM) than in WT cells (0.1 and 0.5 µM). Similarly, the mean growth and shrinkage lengths were also increased in cells of both genotypes after OEA treatment, and the same OEA concentration was required (Supplementary Table 2). In contrast, WT microtubules underwent a decrease in the percentage of growing time ($p < 0.05$) and an increase in the percentage of time in pause ($p < 0.05$), whereas no effect on these parameters was seen for *Ccp1*-KO microtubules (Supplementary Table 2). Regarding microtubule structure, OEA did not affect the static curvature of WT microtubules at any concentration (Fig. 9b). Conversely, OEA decreased *Ccp1*-KO microtubule curvature at all the concentrations tested (Fig. 9b; $p < 0.05$ for all analyses), making the microtubules appear similar to WT microtubules. Last, OEA did not seem to affect the curvature of the microtubule trajectory in cells of any genotype (Fig. 9c). These findings suggest that the molecular effect of OEA may be related to microtubule dynamics and structure since OEA influenced these microtubule features in *Ccp1*-KO (PCD-like) cells.

Discussion

In the present work, we explored the neuroprotective effects of the endocannabinoid OEA and its influence on the cerebellar integrity and behavior of PCD mice on C57BL/DBA background strain. Overall, OEA delayed Purkinje cell degeneration and reversed behavioral impairment through the endocannabinoid receptor PPARα in this model of cerebellar neurodegeneration.

PPARα is considered the main target of OEA [35–38]. Its expression was detected in the three layers of the cerebellum in mice of both genotypes. However, in the Purkinje cells of PCD mice, PPARα receptor expression decreased from P15 to P22, indicating that the *pcd* mutation affects the expression of elements of the endocannabinoid system in both the preneurodegenerative and neurodegenerative stages. Changes in PPARα expression may be reflect plasticity of the cerebellum in an attempt to prevent neuronal death, which is in accordance with previous studies [26, 28, 29, 33]. Nevertheless, the detection of PPARα expression in Purkinje cells led us to design an experiment to assess the effects of OEA *in vivo*. Indeed, the administration of OEA to PCD animals increases the expression of PPARα, as previously described [32]. This finding may be related to plasticity of Purkinje cells aimed at preventing neuronal death, which is consistent with the general neuroprotective effects exerted by OEA that we observed in PCD mice. In contrast, the expression of the CB1 and CB2 receptors was not affected. Although a putative effect of OEA on these receptors cannot be excluded, the activity of OEA is considered to be linked to PPARα [33–35, 37], thus supporting our hypothesis (see also the later discussion of the use of the PPARα antagonist GW6471).

OEA altered the *in vitro* dynamics and structure of microtubules in cells of both genotypes, causing microtubules from PCD-like cells to be similar to those from WT cells. Since OEA normalizes some of the microtubule characteristics impaired in the microtubules of PCD-like cells, we speculate that the preventive effect of OEA on Purkinje cell morphology alterations may be related to its crucial effects on cytoskeletal structures within these cells. Previous findings have shown that the binding of OEA to PPARα triggers the expression of different proteins (i.e., MAP-2 and GAP-43) that are related to microtubule stability and structure and neuronal growth [37]. Thus, the re-establishment of PCD microtubule shape by OEA may reflect the maintenance of the morphology of Purkinje cell dendritic arbors and the prevention of Purkinje cell death in PCD mice. The observed effects of OEA *in vivo* are in line with previous results, both in relation to its pharmacokinetics and effective time window [24, 27, 29, 31]. On the one hand, OEA administration prevents Purkinje cell morphological defects and decreases cell loss when it is administered prior to preneurodegeneration (i.e., chronic administration from P7 to P21 and acute administration at P14, P12 and P10). On the other hand, this neuroprotective effect follows an inverted U-shaped time-response curve, with acute administration at P12 being the most effective treatment, especially regarding dendritic arborization maintenance. Specifically, abnormalities in neural arborization are associated with numerous neurological disorders, such as schizophrenia, epilepsy, Alzheimer's disease and autism spectrum disorder [48–51, 52]. Hence, our findings highlight the potential therapeutic use of OEA as a neuroprotective drug, not only for cerebellar diseases.

Although the cerebellum has long been considered to be a purely motor structure, recent studies have revealed that it also plays an important role in nonmotor functions such as cognitive and affective behavior [14, 17, 18], among others. A previous study conducted in our laboratory demonstrated that cerebellar degeneration at an early age in PCD mice leads to motor, cognitive and social alterations [14, 19, 20], mimicking

the features of human neurodevelopmental disorders in which the cerebellum is involved [7, 18, 21]. It is important to consider that impairments in PCD behavior take place when morphological alterations in Purkinje cells are exacerbated or when these cells are lost, and no other brain regions or neural cell population are affected [14, 53–55]. Thus, the effect of OEA in stabilizing Purkinje cell arborization and increasing Purkinje cell survival should result in functional improvements. Indeed, the results of this study revealed that OEA ameliorated all the behavioral defects observed in the PCD mutant mice until P30, which is in agreement with the histological findings. The results of the *rotarod* test show that the general motor behavior of the treated PCD mice was halfway between that of the WT and untreated PCD mice from P22 to P40. However, the improvements observed in WT mice from P30 onward due to learning [56] was not detected in treated mice. The divergent motor behavior translated into a different trajectory curve in the graph would explain the interaction observed between the analyzed factors. These findings revealed that the neuroprotective effects exerted by OEA at both morphological and cell survival levels contributed to improve the motor task performance of the PCD mice although they were not enough to completely restore its motor defects. Regarding overall behavior, our results are in agreement with previous studies showing that general cerebellar degeneration is manifested as changes in the time spent in grooming, rearing, exploration and displacement [14, 19, 20, 57, 58]. In this sense, the administration of OEA led to reestablishing normal behavioral patterns, with treated PCD mice exhibiting behavior similar to that of WT animals up to P30. In our study, no hypolocomotor effects related to high doses of OEA were observed [29, 40, 59]. In addition, it was recently found that normal cognitive and social abilities require normal cerebellar activity [14, 17, 18, 60, 61]. In this context, the results obtained in the NOR and social preference tests revealed that OEA protects against the impairments observed in the mouse model of cerebellar degeneration employed in this study. These findings are in agreement with those of other studies in which other endocannabinoids mainly restored or improved cognitive function in different mouse models of brain damage [25, 32, 62–65]. Furthermore, it should be noted that, as far as we know, our study is the first to show that OEA has the effect of maintaining normal social behavior in mice with affective deficits related to cerebellar dysfunction.

Overall, OEA was observed to have a neuroprotective effect at both the histological and behavioral levels until P30. Although the changes in two of the five parameters measured were maintained at P40 at the histological level (soma area and primary dendrite length), this was not the case for any behavioral changes. In addition, it should be noted that motor impairments in PCD mice at this age could be responsible for the results obtained in the memory and the social preference tests at P40; therefore, no conclusive results can be drawn. Regardless of this, it is important to note that we managed to delay the degeneration in PCD mice and increase the temporal window in which other therapeutic approaches could be employed synergistically to fight against rapid and aggressive neurodegeneration [58, 66, 67].

Finally, the neuroprotective effects of OEA treatment in PCD mice were mainly mediated by PPARα since the administration of the PPARα antagonist GW6471 fully reversed the OEA-mediated effects at both the cellular and behavioral levels. In the particular case of Purkinje cell survival, our results showed that the inhibition of PPARα before OEA treatment not only abolished the preventive effect of OEA but also increased Purkinje cell death. This finding may be related to apoptosis since PPARα inhibition can promote programmed cell death [68]. Although we cannot discard a direct or indirect effect on other different neural cell types and/or the implication of other molecular interactions [29, 69, 70], our findings confirm the direct involvement of PPARα [36–38] in the neuroprotective effects of OEA observed in this study. Indeed, these results are consistent with the absence of changes in the expression of other classical endocannabinoid receptors in PCD mice.

In conclusion, although the molecular mechanism underlying the effect of OEA requires further study, its neuroprotective effect is apparent at both the histological and behavioral levels. This neuroprotective effect may be related to the re-establishment of cytoskeletal properties and the ensuing maintenance of the structure of Purkinje cells in the cerebellum and, therefore, improvements in impaired behavioral functions. These findings provide evidence supporting the clinical use of OEA as a potential pharmacological molecule for limiting severe neurodegenerative processes.

Supplementary Information The online version contains supplementary material available at https://doi.org/10.1007/s13311-021-01044-3.

Acknowledgements The authors would like to thank the zootechnicians of the Grenoble Institute Neuroscience (GIN) and express their gratitude to M. J. Sánchez-Domínguez for technical support.

Required Author Forms Disclosure forms provided by the authors are available with the online version of this article.

Author Contribution EPM, RMC, DD, MJM, AA, JRA, and EW conceived the study and designed the experiments; EPM and RMC performed the *in vivo* experiments; EPM performed and analyzed the behavioral tests; EPM, RMC, and CdP performed the histological analyses; RMC and MJM performed the *in vitro* experiments; RMC and JMMC performed the mathematical analyses of microtubule curvature; EPM, RMC, CCAZ, JRA, DD, and EW interpreted the results; and EPM was a major contributor to the writing of the paper and organization and design of all the figures. All the coauthors revised and approved the final manuscript.

Funding This work was supported by the Ministry of Economy, Industry and Competitiveness (MINECO) (SAF2016-79668-R to EW), the Ministry of Science and Innovation (PID2019-106943RB-I00 to EW), the Ministry of Science and Innovation/Universities (MICINN/MIU) (FPU16/04259 to EPM; FPU14/02963 to CdP), the Regional Government of Castile and Leon (SA178U13 to EW), the Centre for Regenerative Medicine and Cell Therapy of Castile and Leon (EW), the University of Salamanca (EW), Inserm, University Grenoble Alpes, CNRS, CEA, La Ligue Contre le Cancer Comité de l'Isère (MJM), and Fondation France Alzheimer (to MJM).

Declarations

Conflict of Interest The authors declare that they have no competing interests.

References

1. Andrieux A, Salin PA, Vernet M, et al. The suppression of brain cold-stable microtubules in mice induces synaptic defects associated with neuroleptic-sensitive behavioral disorders. Genes Dev. 2002;16(18):2350–2364.
2. Feinstein SC, Wilson L. Inability of tau to properly regulate neuronal microtubule dynamics: A loss-of-function mechanism by which tau might mediate neuronal cell death. Biochim Biophys Acta. 2005;1739(2–3):268–279.
3. Fu X, Brown KJ, Yap CC, Winckler B, Jaiswal JK, Liu JS. Doublecortin (Dcx) family proteins regulate filamentous actin structure in developing neurons. J Neurosci. 2013;33(2):709–721.
4. Volle J, Brocard J, Saoud M, et al. Reduced expression of STOP/MAP6 in mice leads to cognitive deficits. Schizophr Bull. 2013;39(5):969–978.
5. Eira J, Silva CS, Sousa MM, Liz MA. The cytoskeleton as a novel therapeutic target for old neurodegenerative disorders. Prog Neurobiol. 2016;141:61–82.
6. Matamoros AJ, Baas PW. Microtubules in health and degenerative disease of the nervous system. Brain Res Bull. 2016;126:217–225.
7. Shashi V, Magiera MM, Klein D, et al. Loss of tubulin deglutamylase CCP1 causes infantile-onset neurodegeneration. EMBO J. 2018;37(23):e100540.
8. Breuss M, Keays DA. Microtubules and neuro developmental disease: The movers and the makers. Adv Exp Med Biol. 2014;800:75–96.
9. Magiera MM, Bodakuntla S, Žiak J, et al. Excessive tubulin polyglutamylation causes neurodegeneration and perturbs neuronal transport. EMBO J. 2018;37(23):e100440.
10. Rogowski K, Van Dijk J, Magiera MM, et al. A family of protein-deglutamylating enzymes associated with neurodegeneration. Cell. 2010;143(4):564–578.
11. Baird FJ, Bennett CL. Microtubule Defects & Neurodegeneration. J Genet Syndr Gene Ther. 2013;04(11):203.
12. Bosch Grau M, Masson C, Gadadhar S, et al. Alterations in the balance of tubulin glycylation and glutamylation in photoreceptors leads to retinal degeneration. J Cell Sci. 2017;130(5):938–949.
13. Li J, Snyder EY, Tang FHT, Pasqualini R, Arap W, Sidman RL. Nna1 gene deficiency triggers Purkinje neuron death by tubulin hyperglutamylation and ER dysfunction. JCI Insight. 2020;5(19):e136078.
14. Muñoz-Castañeda R, Díaz D, Peris L, et al. Cytoskeleton stability is essential for the integrity of the cerebellum and its motor- and affective-related behaviors. Sci Rep. 2018;8(1):3072.
15. Valero J, Berciano MT, Weruaga E, Lafarga M, Alonso JR. Preneurodegeneration of mitral cells in the pcd mutant mouse is associated with DNA damage, transcriptional repression, and reorganization of nuclear speckles and Cajal bodies. Mol Cell Neurosci. 2006;33(3):283–295.
16. Baltanás FC, Casafont I, Lafarga V, et al. Purkinje cell degeneration in pcd mice reveals large scale chromatin reorganization and gene silencing linked to defective DNA repair. J Biol Chem. 2011;286(32):28287–28302.
17. Badura A, Verpeut JL, Metzger JW, et al. Normal cognitive and social development require posterior cerebellar activity. Elife. 2018;7:1–36.
18. Carta I, Chen CH, Schott AL, Dorizan S, Khodakhah K. Cerebellar modulation of the reward circuitry and social behavior. Science . 2019;363(6424):eaav0581.
19. Lalonde R and Strazielle C. Spontaneous and induced mouse mutations with cerebellar dysfunctions: behavior and neurochemistry. Brain Research. 2007;1140: 51-74.
20. Lalonde R, Manseau M and Botez MI. Exploration and habituation in Purkinje cell degeneration mutant mice. Brain Research. 1989;479:201-203.
21. Sheffer R, Gur M, Brooks R, et al. Biallelic variants in AGTPBP1, involved in tubulin deglutamylation, are associated with cerebellar degeneration and motor neuropathy. Eur J Hum Genet. 2019;27:1419-1426.
22. Parolaro D, Realini N, Vigano D, Guidali C, Rubino T. The endocannabinoid system and psychiatric disorders. Exp Neurol. 2010;224(1):3–14.
23. Rossi S, Bernardi G, Centonze D. The endocannabinoid system in the inflammatory and neurodegenerative processes of multiple sclerosis and of amyotrophic lateral sclerosis. Exp Neurol. 2010;224(1):92–102.
24. Viscomi MT, Oddi S, Latini L, Bisicchia E, Maccarrone M, Molinari M. The endocannabinoid system: A new entry in remote cell death mechanisms. Exp Neurol. 2010;224(1):56–65.
25. Holubiec MI, Romero JI, Suárez J, et al. Palmitoylethanolamide prevents neuroinflammation, reduces astrogliosis and preserves recognition and spatial memory following induction of neonatal anoxia-ischemia. Psychopharmacology (Berl). 2018;235(10):2929–2945.
26. Galán-Rodríguez B, Suárez J, González-Aparicio R, et al. Oleoylethanolamide exerts partial and dose-dependent neuroprotection of substantia nigra dopamine neurons. Neuropharmacology. 2009;56(3):653–664.
27. Flores JA, Galán-Rodríguez B, Rojo AI, Ramiro-Fuentes S, Cuadrado A, Fernández-Espejo E. Fibroblast growth factor-1 within the ventral tegmental area participates in motor sensitizing effects of morphine. Neuroscience. 2010;165(1):198–211.
28. González-Aparicio R, Blanco E, Serrano A, et al. The systemic administration of oleoylethanolamide exerts neuroprotection of the nigrostriatal system in experimental Parkinsonism. Int J Neuropsychopharmacol. 2014;17(3):455–468.
29. González-Aparicio R, Moratalla R. Oleoylethanolamide reduces L-DOPA-induced dyskinesia via TRPV1 receptor in a mouse model of Parkinson's disease. Neurobiol Dis. 2014;62:416–425.
30. Joshi U, Evans JE, Joseph R, et al. Oleoylethanolamide treatment reduces neurobehavioral deficits and brain pathology in a mouse model of Gulf War Illness. Sci Rep. 2018;8(1):1–15.
31. Romano A, Micioni Di Bonaventura MV, Gallelli CA, et al. Oleoylethanolamide decreases frustration stress-induced binge-like eating in female rats : a novel potential treatment for binge eating disorder. Neuropsychopharmacology. 2020;45:1931–1941.
32. Yang LC, Guo H, Zhou H, et al. Chronic oleoylethanolamide treatment improves spatial cognitive deficits through enhancing hippocampal neurogenesis after transient focal cerebral ischemia. Biochem Pharmacol. 2015;94(4):270–281.
33. Sayd A, Antón M, Alén F, et al. Systemic administration of oleoylethanolamide protects from neuroinflammation and

anhedonia induced by LPS in rats. Int J Neuropsychopharmacol. 2016;19(3): pyw004.
34. Zhou Y, Yang LC, Ma A, et al. Orally administered oleoylethanolamide protects mice from focal cerebral ischemic injury by activating peroxisome proliferator-activated receptor α. Neuropharmacology. 2012;63(2):242–249.
35. Fu J, Gaetani S, Oveisi F, et al. Oleylethanolamide regulates feeding and body weight through activation of the nuclear receptor PPAR-alpha. Nature. 2003;425(6953):90–93.
36. Genovese T, Mazzon E, Di Paola R, et al. Role of endogenous ligands for the peroxisome proliferators activated receptors alpha in the secondary damage in experimental spinal cord trauma. Exp Neurol. 2005;194(1):267–278.
37. Guzmán M, Lo Verme J, Fu J, Oveisi F, Blázquez C, Piomelli D. Oleoylethanolamide stimulates lipolysis by activating the nuclear receptor peroxisome proliferator-activated receptor alpha (PPAR-alpha). J Biol Chem. 2004;279(27):27849–27854.
38. Fu J, Oveisi F, Gaetani S, Lin EB, Piomelli D. Oleoylethanolamide, an endogenous PPAR-α agonist, lowers body weight and hyperlipidemia in obese rats. Neuropharmacology. 2005;48:1147–1153.
39. Bento-Abreu A, Tabernero A, Medina JM. Peroxisome proliferator-activated receptor-alpha is required for the neurotrophic effect of oleic acid in neurons. J Neurochem. 2007;103(3):871–881.
40. Fedele S, Arnold M, Krieger JP, et al. Oleoylethanolamide-induced anorexia in rats is associated with locomotor impairment. Physiol Rep. 2018;6(3):e13517.
41. Ennaceur A. One-trial object recognition in rats and mice: methodological and theoretical issues. Behav Brain Res. 2010;215(2):244–254.
42. Ennaceur A, Delacour J. A new one-trial test for neurobiological studies of memory in rats. III. Spatial vs. non-spatial working memory. Behav Brain Res. 1988;31(1):47–59.
43. Antunes M, Biala G. The novel object recognition memory: neurobiology, test procedure, and its modifications. Cogn Process. 2012;13:93–110.
44. Moy SS, Nadler JJ, Perez A, et al. Sociability and preference for social novelty in five inbred strains: an approach to assess autistic-like behavior in mice. Genes, Brain Behav. 2004;3(5):287–302.
45. Erck C, Peris L, Andrieux A, et al. A vital role of tubulin-tyrosine-ligase for neuronal organization. Proc Natl Acad Sci. 2005;102(22):7853–7858.
46. Peris L, Wagenbach M, Lafanechère L, et al. Motor-dependent microtubule disassembly driven by tubulin tyrosination. J Cell Biol. 2009;185(7):1159–1166.
47. Applegate KT, Besson S, Matov A, Bagonis MH, Jaqaman K, Danuser G. PlusTipTracker: Quantitative image analysis software for the measurement of microtubule dynamics. J Struct Biol. 2011;176(2):168–184.
48. Bernardinelli Y, Nikonenko I, Muller D. Structural plasticity: mechanisms and contribution to developmental psychiatric disorders. Front Neuroanat. 2014;8:1–9.
49. Bourgeron T. From the genetic architecture to synaptic plasticity in autism spectrum disorder. Nat Rev Neurosci. 2015;16(9):551–563.
50. Tampellini D. Synaptic activity and Alzheimer's disease: A critical update. Front Neurosci. 2015;9:1–7.
51. Wu Y, Liu D, Song Z. Neuronal networks and energy bursts in epilepsy. Neuroscience. 2015;287:175–186.
52. Rojek KO, Krzemień J, Doleżyczek H, et al. Amot and Yap1 regulate neuronal dendritic tree complexity and locomotor coordination in mice. PLOS Biol. 2019;17(5):e3000253.
53. Mullen RJ, Eicher EM, Sidman RL. Purkinje cell degeneration: a new neurological mutation in the mouse. Proc Natl Acad Sci USA. 1976;208–212.
54. Wang T, Morgan JI. The Purkinje cell degeneration (pcd) mouse: an unexpected molecular link between neuronal degeneration and regeneration. Brain Research. 2007;1140:26-40.
55. Baltanás FC, Berciano MT, Valero J, et al. Differential glial activation during the degeneration of Purkinje cells and mitral cells in the PCD mutant mice. Glia. 2013;61(2):254-272.
56. Buitrago MM, Schulz JB, Dichgans J, Luft AR. Short and long-term motor skill learning in an accelerated rotarod training paradigm. Neurobiol Learn Mem. 2004;81(3):211–216.
57. Strazielle C, Lalonde R. Grooming in Lurcher mutant mice. Physiol Behav. 1998;64(1):57–61.
58. Díaz D, Piquer-Gil M, Recio JS, et al. Bone marrow transplantation improves motor activity in a mouse model of ataxia. J Tissue Eng Regen Med. 2018;12(4):e1950–1961.
59. De Fonseca Rodríguez F, Navarro M, Gómez R, et al. An anorexic lipid mediator regulated by feeding. Nature. 2001;414:209–212.
60. Passot JB, Sheynikhovich D, Duvelle É, Arleo A. Contribution of cerebellar sensorimotor adaptation to hippocampal spatial memory. PLoS One. 2012;7(4):42–46.
61. Tsai PT, Hull C, Chu Y, et al. Autistic-like behaviour and cerebellar dysfunction in Purkinje cell Tsc1 mutant mice. Nature. 2012;488:647–651.
62. Campolongo P, Roozendaal B, Trezza V, et al. Fat-induced satiety factor oleoylethanolamide enhances memory consolidation. Proc Natl Acad Sci. 2009;106(19):8027–8031.
63. Mazzola C, Medalie J, Scherma M, et al. Fatty acid amide hydrolase (FAAH) inhibition enhances memory acquisition through activation of PPAR-alpha nuclear receptors. Learn Mem. 2009;16(5):332–337.
64. D'Agostino G, Russo R, Avagliano C, Cristiano C, Meli R, Calignano A. Palmitoylethanolamide protects against the amyloid-B25-35-induced learning and memory impairment in mice, an experimental model of alzheimer disease. Neuropsychopharmacology. 2012;37(7):1784–1792.
65. Mirza R, Sharma B. Selective modulator of peroxisome proliferator-activated receptor-α protects propionic acid induced autism-like phenotypes in rats. Life Sci. 2018;214:106–117.
66. Recio JS, Álvarez-Dolado M, Díaz D, et al. Bone marrow contributes simultaneously to different neural types in the central nervous system through different mechanisms of plasticity. Cell Transplant. 2011;20(8):1179–1192.
67. Díaz D, del Pilar C, Carretero J, Alonso JR, Weruaga E. Daily bone marrow cell transplantations for the management of fast neurodegenerative processes. J Tissue Eng Regen Med. 2019;13(9):1702–1711.
68. Abu Aboud O, Wettersten HI, Weiss RH. Inhibition of PPARα Induces Cell Cycle Arrest and Apoptosis, and Synergizes with Glycolysis Inhibition in Kidney Cancer Cells. PLoS One. 2013;8(8):1–9.
69. Proulx K, Cota D, Castañeda TR, et al. Mechanisms of oleoylethanolamide-induced changes in feeding behavior and motor activity. Am J Physiol Regul Integr Comp Physiol. 2005;289(3):R729–737.
70. Kim SR, Chung YC, Chung ES, et al. Roles of transient receptor potential vanilloid subtype 1 and cannabinoid type 1 receptors in the brain: Neuroprotection versus neurotoxicity. Mol Neurobiol. 2007;35(3):245–254.